

# The Fabrication of Scintillator Column by Hydraulic Pressure Injection Method

C. C. Chen, C. M. Chu, C. J. Wang, C. Y. Chen, K. J. Huang

**Abstract**—Cesiumiodide with Na doping (CsI(Na)) solution or melt is easily forming three- dimension dendrites on the free surface. The defects or bobbles form inside the CsI(Na) during the solution or melt solidification. The defects or bobbles can further effect the x-ray path in the CsI(Na) crystal and decrease the scintillation characteristics of CsI(Na). In order to enhance the CsI(Na) scintillated property we made single crystal of CsI(Na) column in the anodic aluminum oxide (AAO) template by hydraulic pressure injection method. It is interesting that when CsI(Na) melt is confined in the small AAO channels, the column grow as stable single column without any dendrites. The high aspect ratio (100~10000) of AAO and nano to sub-micron channel structure which is a suitable template for single of crystal CsI(Na) formation. In this work, a new low-cost approach to fabricate scintillator crystals using anodic aluminum oxide (AAO) rather than Si is reported, which can produce scintillator crystals with a wide range of controllable size to optimize their performance in X-ray detection.

**Keywords**—Cesiumiodide, AAO, scintillator, crystal, X-ray.

## I. INTRODUCTION

X RAY detection devices for an X-ray image pickup having an X-ray digital radiography system, there is a device in which a sensor panel and a scintillator are adhered to each other through an adhesion layer made of a transparent adhesive [1]-[4]. Cesium iodide (CsI) used in the phosphor layer of a scintillator plate exhibits a relatively high conversion rate of from X-ray to visible light [5]-[8]. A technique for use as an X-ray phosphor in which a mixture of CsI and sodium iodide (NaI) at any mixing ratio deposit on the glass substrate to form sodium-activated cesium iodide (CsI:Na), which was further subjected to annealing as a post-treatment to achieve enhanced visible-conversion efficiency [9]-[11].

As described in Chen [12], AAO film can be fabricated using an anodization process. The fabrication process for 15nm AAO template consists are following steps:

(a) Polish the aluminum (Al) substrate (99.7%); then anneal in an air furnace at 550°C; (b) Electro-polish the substrate in a bath consisting of  $\text{HClO}_4$ ,  $\text{C}_2\text{H}_6\text{O}$ , and  $\text{CH}_3(\text{CH}_2)_3\text{OCH}_2\text{CH}_2\text{OH}$  with 42 V for 10 minutes; (c) First anodization – Polish the Al substrate with 18 V DC in  $\text{H}_2\text{SO}_4$  solution for 20 minutes; (d) Remove the first anodization film by soaking in a solution of

$\text{CrO}_3$  and  $\text{H}_3\text{PO}_4$  for 40 minutes; (e) Second anodization – Repeat anodization using the solution from the first anodization, but for a longer time (several hours) to form AAO films of varying thickness; (f) Remove Al substrate by soaking in a solution of  $\text{CuCl}_2$  and  $\text{HCl}$  for 30 minutes; (g) Widen pore diameter of AAO template using  $\text{H}_3\text{PO}_4$  solution and 40 V for 20 minutes.

From the above steps, we can conclude that by varying parameter values such as voltage, time, and solution, AAO film of different sizes, pore diameter, and thickness can be produced. For example, (a) AAO with 10nm to 25nm pore size and 10 $\mu\text{m}/\text{h}$  film growth rate can be made by anodization of 10 vol.%  $\text{H}_2\text{SO}_4$  electrolyte and 18V applied voltage, (b) AAO with 30nm to 90nm pore size and 8 $\mu\text{m}/\text{h}$  film growth rate can be made by anodization of 3 wt.%  $\text{C}_2\text{H}_2\text{O}_4$  electrolyte and 40V applied voltage, (c) AAO with 180nm to 500nm pore size and 5  $\mu\text{m}/\text{h}$  film growth rate can be made by anodization of 1 vol.%  $\text{H}_3\text{PO}_4$  electrolyte and 195 V applied voltage. AAO can have various pore sizes and pore densities; for example, (a) 10nm pore size, with pore density of  $8.4 \times 10^{10}$  pores. $\text{cm}^{-2}$ , (b) 50nm pore size, with pore density of  $1.3 \times 10^{10}$  pores. $\text{cm}^{-2}$ , (c) 250nm pore size, with pore density of  $1.2 \times 10^9$  pores. $\text{cm}^{-2}$ , (d) 500nm pore size, with pore density of  $4.5 \times 10^8$  pores. $\text{cm}^{-2}$ .

Since a regular scintillator has no function to guide the path of x-ray through, partitions functioning as a scattering surface and/or a reflection surface are required. In this paper, we provided a structure which has a function to guide the path of x-ray into Charge Coupled Device (CCD).

## II. EXPERIMENTAL PROCEDURE

The starting materials are CsI powder, NaI powder, and high-purity Al foil. The Al foil was then through anodization formation AAO template. And, 1 mole CsI + 0.03 mole NaI mixing powder was then through shaping and sintering formation CsI (Na) ingot. In order to observe the CsI (Na) column inside AAO template the following experiment steps were needed. (1) CsI (Na) ingot put on the AAO surface, (2) heating CsI (Na)/AAO at 630 °C, applied a hydraulic pressure (100 kgf/ $\text{cm}^2$ ) to the CsI (Na) melt, (3) cooling CsI (Na)/AAO sample at 30°C/min of cooling rate. According to above steps we can obtain the CsI (Na) nano or sub-micron CsI (Na) column.

Because the size and quality of CsI (Na) column were controlling based on the AAO the high quality of AAO template was needed. AAO templates with a pore size of 10 to 500 nm were generated by Al foil in acid solutions of sulfuric acid ( $\text{H}_2\text{SO}_4$ ), oxalic acid ( $\text{COOH}$ ) $_2$ , or phosphoric acid ( $\text{H}_3\text{PO}_4$ ).

C.C. Chenr, C.M. Chur, C.J. Wangr, C.Y. Chenr is with the Department of Energy Engineering, National United University, Miaoli, Taiwan (phone: +886-37-382383; fax:+886-37-382-39; e-mail: ccchen@nuu.edu.tw, poiuytrewq7191@gmail.com, egg00135@gmail.com, d92527002@ntu.edu.tw).

K.J. Huangr is with the Chung-Shan Institute of Science and Technology, Taoyuan 325, Taiwan (e-mail: kjhuang@gmail.com).

The pre-treatment of Al substrate were through mechanical grounding with #2000 SiC paper, annealing at 550°C for 1 hr, electro-polished at 42 volts (DC) applied for 10 min.

A 20 nm pore diameter template was then fabricated by anodizing the polished-Al substrate at 18V in 10 vol.%  $\text{H}_2\text{SO}_4$  at 15°C for 20 min. Similar to the above process, for 40nm pore diameter  $\text{Al}_2\text{O}_3$  NT template, the electrolyte was 3 vol.%  $(\text{COOH})_2$  at 25°C, and the applied voltage was 40 V. For 500nm pore diameter AAO template, the electrolyte was 1 vol.%  $\text{H}_3\text{PO}_4$  at 0°C, and the applied voltage was 200 V. The time of pore widening was 200min.

### III. RESULTS AND DISCUSSION

When anodized in an acidic electrolyte and controlled under suitable conditions, aluminum forms a porous oxide called anodic aluminum oxide (AAO) with very uniform and parallel cell pores. Since AAO process is sensitive to the operation conditions, defects would appear on AAO when an unsuitable condition was used. The conditions include electrolyte temperature, surrounding temperature while AAO process is finished, applied voltage, electrolyte composition, chemical etching, and stable current density. In the several years of our experience, we can make high quality AAO template.

Fig. 1 showed photographs of step by step of AAO sample fabrication; (a) 0.3mm thickness, 4 inch diameter, 99.999% purity aluminum foil as AAO substrate, (b) the substrate through mechanical polishing, (c) electrolytic polishing, (d) 1st anodization, (e) ordering pattern formation on the substrate after removed the 1st anodization layer, (f) 2nd anodization, (g) and (h) suitable sample size after cutting, (i) AAO film without Al substrate. Fig. 2 showed the AAO formation by 1 vol. %  $\text{H}_3\text{PO}_4$  electrolyte, 195V, at -1°C. The microstructure of (a) SEM image with 400 nm diameter and (b) EDS spectrum with composition of Al (53.5 wt.%), O (43.1 wt.%), and P (3.4 wt.%).

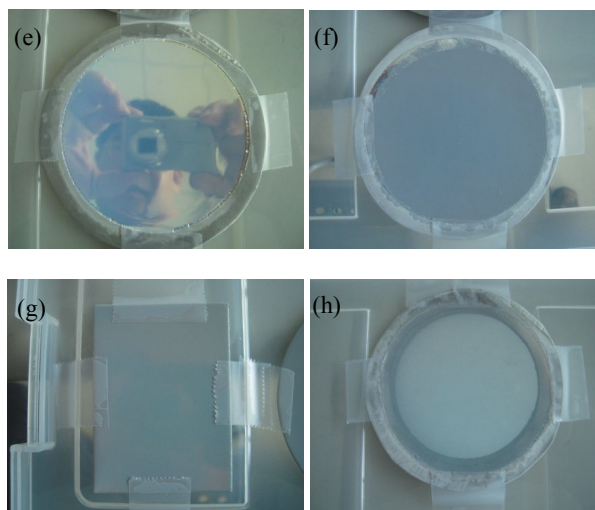


Fig. 1 Photographs of step by step of AAO sample fabrication; (a) aluminum foil, (b) Al through mechanical polishing, (c) electrolytic polishing, (d) 1<sup>st</sup> anodization, (e) ordering pattern, (f) 2<sup>nd</sup> anodization, (g) and (h) suitable sample size

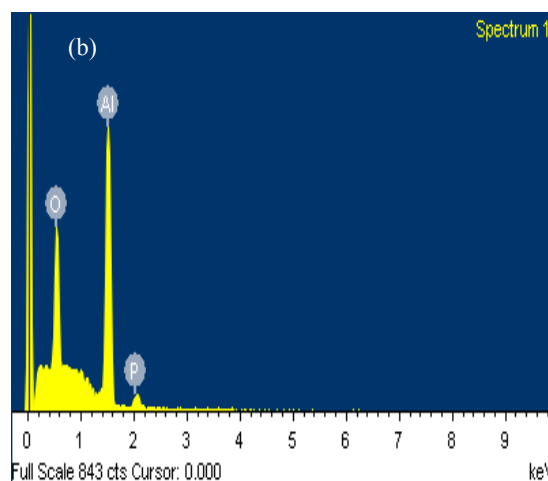
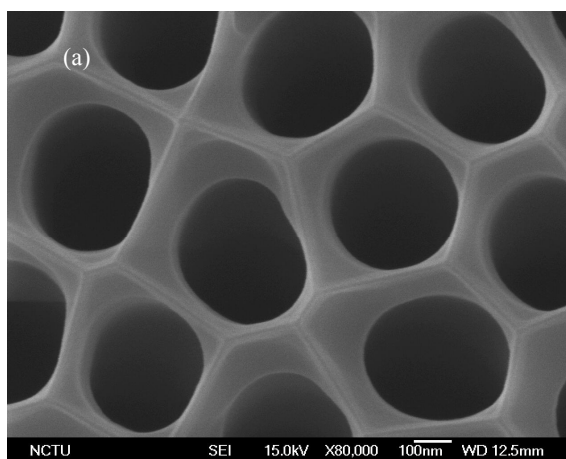


Fig. 2 AAO micro-information of (a) SEM image and (b) EDS spectrum

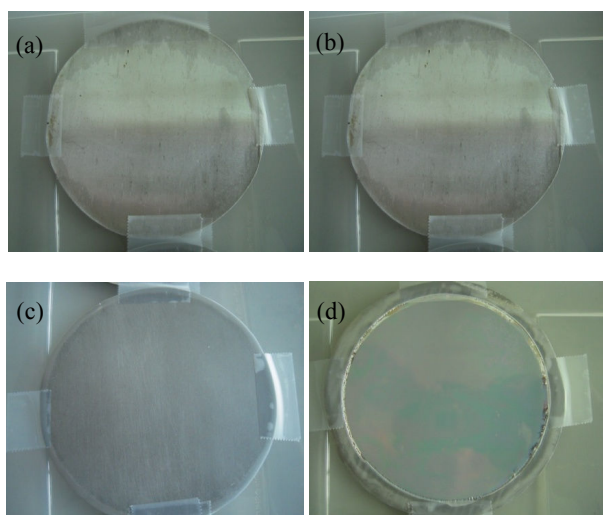


Fig. 3 showed CsI (Na) was fabricated by a (a) hydraulic pressure method forming CsI (Na) ingot. (b) In order to enhance the mechanical properties and homogeneous of Na in CsI the ingot was then through sintering in the vacuum quiz tube. (c) The CsI (Na) column can therefore form inside AAO template when the source material of CsI (Na) ingot put on the AAO surface at 630°C and applied a hydraulic pressure on. Fig. 4 Photographs of (a) vacuum injecting chamber, (b) a vacuum injecting chamber set on the hydraulic equipment, (c) CsI (Na) column inside AAO template. The diameter and length of CsI (Na) are depended on the AAO size; in this case, the CsI (Na) columns have about 500nm diameter and 100µm length.

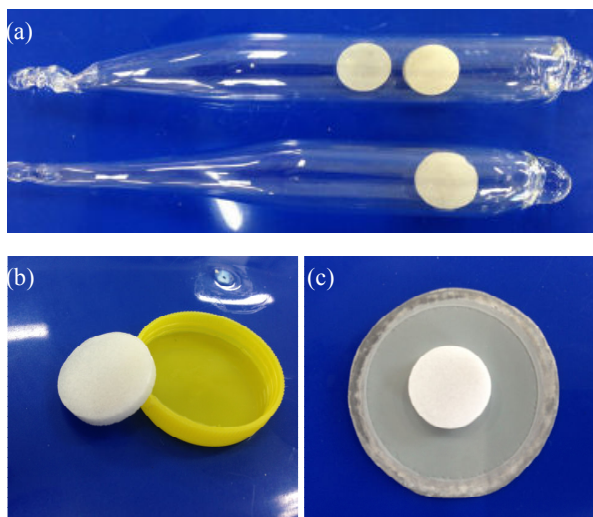


Fig. 3 Photographs of (a) CsI (Na) ingot, (b) sintering of ingot in the vacuum quiz tube, (c) CsI (Na) ingot put on the AAO surface

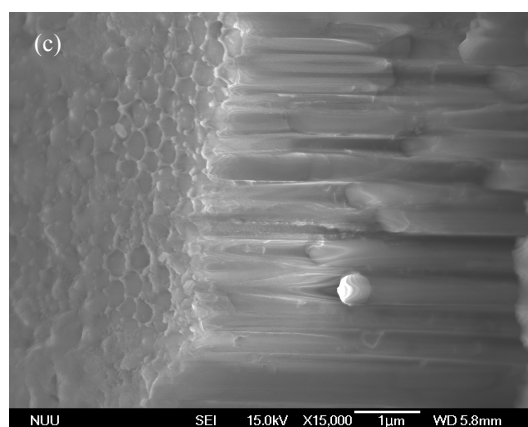
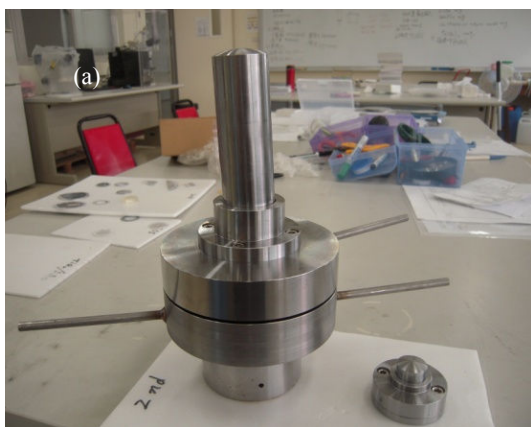


Fig. 4 Photographs of (a) vacuum injecting chamber, (b) a vacuum injecting chamber set on the hydraulic equipment, and (c) CsI (Na) column inside AAO template

#### IV. CONCLUSIONS

In this paper, we provided an ordering structure of scintillator and fabrication method, including: fabricated template with an ordering nano or sub-micron channel by anodization, filled scintillated melt into the template formation single crystal nano or sub-micron crystalline scintillator after solidification.

#### ACKNOWLEDGMENT

The authors gratefully appreciate the financial support of the National Science Council of ROC under the contract No. 102-2221-E-239-008-. This work was financially supported by the Chung- Shan Institute of Science and Technology (CSIST) under the contract No. CSIST-442-V302.

#### REFERENCES

- [1] V.V. Nagarkar, S.V. Tipnis, V. Gaysinskiy, S.R. Miller, I. Shestakova, High-speed digital radiography using structured CsI screens, Nuclear Instruments and Methods in Physics Research Section B: Beam Interactions with Materials and Atoms, 213, (2004) 476-480.
- [2] P. Magnan, Detection of visible photons in CCD and CMOS: A comparative view, Nuclear Instruments and Methods in Physics Research Section A: Accelerators, Spectrometers, Detectors and Associated Equipment, 504(1-3), (2003) 199-212.

- [3] C.M. Schaefer-Prokop, D.W. De Boo, M. Uffmann, M. Prokop. DR and CR: Recent advances in technology, *European Journal of Radiology*, 72(2), (2009) 194-201.
- [4] A. Koch, C. Raven, P. Spanne, A. Snigirev, X-ray imaging with submicrometer resolution employing transparent luminescent screens, *Journal of the Optical Society of America A*, 15(7), (1998) 1940-1951.
- [5] S Zazubovich. Physics of halide scintillators, *Radiation Measurements*, 33(5), (2001) 699-704.
- [6] U.L. Olsen, X. Badel, J. Linnros, M. Di Michiel, T. Martin, S. Schmidt, H.F. Poulsen, Development of a high-efficiency high-resolution imaging detector for 30–80 keV X-rays, *Nuclear Instruments and Methods in Physics Research Section A: Accelerators, Spectrometers, Detectors and Associated Equipment*, 576(1), (2007) 52-55.
- [7] A. M. Gurvich, Luminescent screens for mammography, *Radiation Measurements*, 24(4), (1995) 325-330.
- [8] A Koch, H Rosenfeldt, Powder-phosphor screens combined with interference filters for X-ray imaging with increased brightness, *Nuclear Instruments and Methods in Physics Research Section A: Accelerators, Spectrometers, Detectors and Associated Equipment*, 432(2-3), (1999) 358-363.
- [9] C. Raven, A. Snigirev, I. Snigireva, P. Spanne, A. Souvorov, and V. Kohn, Phase-contrast microtomography with coherent high-energy synchrotron x rays, *Applied Physics Letters*, 69(13), (1996) 1826-1828.
- [10] A. Lempicki, C. Brecher, P. Szupryczynski, H. Lingertat, V. V. Nagarkar, S. V. Tipnis, and S. R. Miller, A new lutetia-based ceramic scintillator for X-ray imaging, *Nuclear Instruments and Methods in Physics Research Section A: Accelerators, Spectrometers, Detectors and Associated Equipment*, 488(3), (2002) 579-590.
- [11] E. Zych, C. Brecher, and H. Lingertat, Depletion of high-energy carriers in YAG optical ceramic materials, *Spectrochimica Acta Part A: Molecular and Biomolecular Spectroscopy*, 54(11), (1998) 1771-1777.
- [12] C.C. Chen, D. Fang, Z. Luo, Fabrication and Characterization of Highly-Ordered Valve-Metal Oxide Nanotubes and Their Derivative Nanostructures, *Review in Nanoscience and Nanotechnology*, 1(2012) 229-256.